Centrifuge modeling of helical piles in stiff clay: installation torque and pore pressure response

Weidong Li, Lijun Deng, Rick Chalaturnyk
Department of Civil and Environmental Engineering, University of Alberta, Edmonton, Canada
Mohamed Abdelaziz, Richard Schmidt
Almita Piling Inc., Edmonton, Canada

ABSTRACT
Installation torque is commonly used to predict the axial capacity of helical piles. Theoretical models for calculating the torque resistance have been developed for piles in cohesive and cohesionless soils. However, uncertainty induced by excess pore pressure during the installation and soil sensitivity still exists. The present research investigated the torque mechanism of helical piles and the pore pressure response to pile installation. A series of centrifuge model tests of helical piles were conducted at the University of Alberta. Helical piles were installed into a stiff and saturated clay at a high g level and then loaded in the axial directions. Pore pressure transducers measured the pore pressure change surrounding the four helical piles. The results show that the excess pore pressure developed instantly during installation but dissipated over approximately 6 days. The long term ultimate axial capacity of the piles was not affected by the pile installation. The installation torque and axial loading resistance were measured by strain gauges installed in the pile shaft. A theoretical model for the torque resistance was proposed based on the clay-pile interaction implied by the excavation after the load tests. The torque measurements verified the proposed model subject to the assumption that the residual undrained shear strength governed the clay-pile adhesion.

1 INTRODUCTION

Helical plates, affixed to the shaft of helical piles, enlarge the end bearing area and facilitate the installation process to make helical piles a great alternative to conventional deep foundation options. The screw-type installation technique has inspired a unique design method by relating the final installation torque to the ultimate axial capacity. Perko (2007) proposed the following equation to describe this design method:

$$K_T = Q_u/T \quad [1]$$

where K_T is the torque factor, Q_u is the axial capacity of helical piles, and T is the final installation torque. Li and Deng (2019) summarized the torque factors obtained in 26 in-situ axial loading tests of helical piles with a wide range of shaft diameters in clay and sand, and included other test results from Tappenden and Sego (2007) and Sakr (2009, 2012). According to Li and Deng (2019), K_T decreased when the shaft diameter increased in general so that a proper K_T value may be obtained from this correlation curve to guide the prediction of axial capacity for a given shaft diameter. However, a deviation of torque factors has also been identified for these helical piles installed into a multi-layered ground. The soil pockets with much lower shear strength underlying the lowermost helices would reduce the bearing capacities while they had no impact on the installation torque. Therefore, the prediction of axial capacity of helical piles usually relies on the failure modes and subsurface investigation. However, the torque method is sometimes the only or more economic approach to adopt in the axial capacity design of helical piles. For instance, in pipeline construction, site investigation throughout the whole length is too costly compared to the torque factor method.

In order to improve the torque method, studies based on theoretical torque models have been conducted. Tsuha and Aoki (2010) measured the installation torque and axial capacity of several model helical piles in sand on centrifuge to verify the theoretical expression of the final installation torque contributed by the shaft-sand friction and helix-sand friction. Residual friction angle was observed to govern the torque resistance. Sakr (2013) proposed a different theoretical expression of the installation torque by including the including sensitivity for cohesive soils, and assumed the soil entrapped in the helix pitch space would behave as a body bounded to the helix thus contributed the torsional friction on its vertical circumference to the total installation torque. The theoretical prediction was verified by their in-situ installation tests. Spagnoli et al. (2018) used the models proposed by Tsuha and Aoki (2010) and Sakr (2013) to conduct a parametric study on the impact of clay sensitivity on the uplift capacity of helical piles in offshore soils. Sensitivity of clay proved to have significant consequences and should be involved in the prediction of installation torques.

The pile behaviour is largely affected by the excess pore water pressure generation and dissipation, namely the soil setup. Lanyi-Bennett and Deng (2019) observed that the excess pore pressure caused by pile installation resulted in a significant reduction of bearing capacity in the instant loading tests. But the axial behavior of piles after the dissipation of excess pore pressure was yet to be investigated.

The present project is aimed to investigate the torque performance of helical piles during installation in clay and the pore pressure response; the results could further infer the performance of helical piles in the field. A series of

centrifuge model tests were conducted at the University of Alberta. The development and dissipation of excess pore pressure caused by the installation of four helical piles were obtained. The effect of excess pore pressure on the quick-loading axial capacity of these piles was assessed. The installation torque vs depth was recorded and compared with the prediction based on the theoretical model proposed in this paper. Clay sensitivity was applied to the prediction process, which produced consistent results with the measurements.

2 A THEORETICAL MODEL

Tsuha and Aoki (2010) simplified the torque model by assuming the helix angle to be a constant throughout its radius, and Sakr (2013) assumed that the soil trapped in the pitch of helix would act as a cylindrical body that shears against the surrounding soil. However, in the present study, the excavation result after the load tests (Figure 1) shows that there was no soil within the helix pitch that moved together with the helix. Therefore the present torque model treats the helix as a “true helix” by including its spiral ascending angle to the horizontal plane over the entire radius. The present model will be verified by the installation torque records obtained from the centrifuge model tests of helical piles.

Figure 1. A model pile extracted from the clay

According to Figure 1, the installation torque is the result of shear stress acting on the blending helices and the rotating shaft (Figure 2). The component T_{bH} is the torque caused by the bearing resistance when the cutting edge of the helix penetrates into the clay. End bearing factors of clay can be used for estimation. However, it has been popular to sharpen this edge to facilitate pile installation therefore T_{bH} is excluded from the present study. As for the rest shear stress based torque components, considering the large relative displacement between the soil and the pile, residual undrained shear strength is expected to be dominant. To be specific about the helix, although the leading helix was penetrating into intact soil, the majority of the leading helix follows into the gap left behind by the cutting edge. In addition, the pile-clay adhesion factor proposed by Tomlinson (1957) is adopted for torque estimation. Equation 2 shows the components of the estimated torque resistance:

$$T = T_s + T_{cH} + T_{sH} \quad [2]$$

$$T_s = \int_0^{l_s} \pi \frac{d^2}{2} \alpha s_{ur} dx \quad [2\text{-a}]$$

$$T_{cH} = \int_0^P \frac{D}{2} t\alpha s_{ur} \cot(\theta\left(\frac{D}{2}\right)) dx \quad [2\text{-b}]$$

$$T_{sH} = \int_{d/2}^{D/2} 2\,r\cos(\theta(r)) \int_0^P \alpha\, s_{ur} \csc(\theta(r)) dx dr \quad [2\text{-c}]$$

where T_s is the torque against the rotation of the pile shaft, T_{cH} is the torque against the rotation of the circumference of the helix/helices, T_{sH} is the torque acting on the upper and lower surfaces of the helix/helices, d is the shaft diameter, D is the helix diameter, l_s is the embedment depth of pile shaft, α is the pile-clay adhesion factor, s_{ur} is the residual undrained shear strength of the model clay, $\theta(x)$ is the ascending angle of the helix along the helix radius

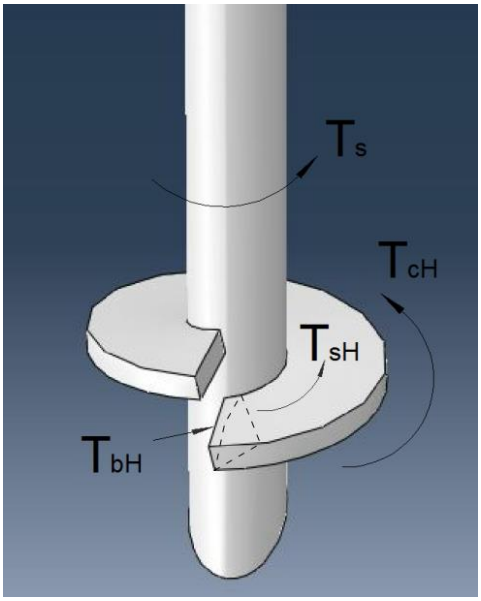

Figure 1. Torque resistance against pile installation

3 CENTRIFUGE MODEL TEST PROGRAM

Eight helical piles were installed in stiff clay on the geotechnical centrifuge at the University of Alberta, and test results of selected piles will be presented in this paper.

Two pore pressure transducers (PPT's) were buried near the final depth of the helices and about 8.7 times of pile shaft radius from each pile axis. Vane shear tests were conducted to obtain the undrained shear strength of the clay. The model helical piles were instrumented with strain gauges to record the installation torques and axial loads. The gravitational acceleration of the centrifuge was set to be 20. The scale factors for the basic engineering units involved in this study are listed in Table 1.

3.1 Model Piles

Two model helical piles (Figure 2) were made of aluminum. Selecting aluminum as the material was to optimize the pile rigidity and magnitude of strain measurements. The model piles were named P1 and P2. The dimensions of the piles are presented in Table 2. Two oppositely positioned strain gauges (SG's) formed each half-bridge circuit to measure the axial strain in the shaft. These half bridge circuits are able to compensate potential minor load inclination. Full-bridge SG circuits were adopted for the measurement installation torque. The SG's in these circuits were placed 45 degrees with regard to the vertical and horizontal directions to compensate any axial strains.

In order to protect the SG's from any potential damages, the torque SG's were covered by Teflon tapes and surrounded by epoxy attachments. Wires were buried in the epoxy near the ends connected to the SG's to avoid any tension in the wired to transfer to the SG's. The axial strain gauges were placed at the bottom of two slots excavated in each pile shaft and then covered with water proof coating, Teflon tape, and epoxy.

3.2 Test Layout

Four axial loading tests including three compression tests and one tension tests are shown in Figure 3. The testing program was divided into two stages: 1) Stage A including two compression tests, i.e., P1C and P2C1; and 2) Stage B including one tension test, P1T, and one compression test, P2C2. The corresponding pile installation was accomplished one day before the load tests to allow the disturbed clay to recover through over-night spinning. The arrangement of the model piles, pore pressure transducers (PPT's), and vane shear boreholes is presented in Figure 3. Each PPT was placed at the center of the two piles near it.

Table 1. Scale factors for basic engineering parameters involved in this study

Quantity	Length	Force	Stress	Torque	Diffusional Time
Prototype/Model	20	400	1	8000	400

Table 2. Pile dimensions

	Pile Type	Number of helix	d (mm)	D (mm)	L (mm)	S (mm)	E (mm)
Model	P1	1	12.7	38.1	271.8	NA.	150
	P2	2	12.7	38.1	271.8	133.4	150
Prototype	P1	1	254	762	5436	NA.	3000
	P2	2	254	762	6436	2668	3000

Note: E is the embedment depth of lower helices, and L is the total length of every pile

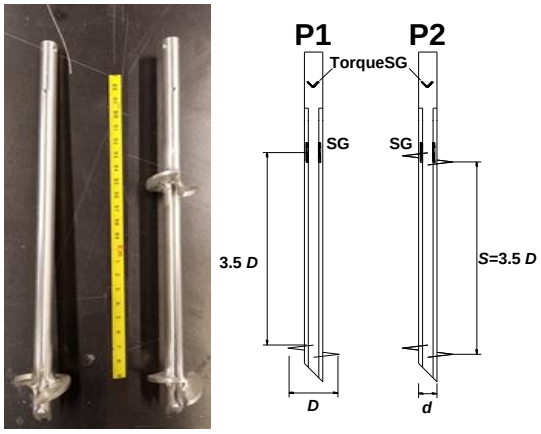

Figure 2. Pile configuration and SG arrangement

3.3 Pore Pressure Transducers

The two pore pressure transducers were installed in the soil at two depths: 10 cm and 15 cm at 1 g condition. To install the PPT, a thin-wall plastic tube with 12.7 mm of external diameter was inserted into the clay to designated depths. Then the tube was pulled out with soil plug inside leaving a vertical borehole behind. The saturated PPT was then pushed into the borehole with the filter side down to reach the bottom. In the end, the soil plug in the tube was extruded with a steel rod to fill back into the borehole. The brass casing of the pore pressure transducer is a cylinder with 10 mm of diameter and 13.5 mm of height. Each transducer weighs 2.3 gm, and its density is 2.17 gm/cm^3, which is slightly greater than the bulk density of the clay (1.81 gm/cm^3). The effect of the differential density between soil and transducers on the excess water pressure was observed to be minimal.

3.4 Soil Properties

The undrained shear strength, s_u, varied with the depth of the clay. The peak and residual strengths at five depths per location were obtained. The results of peak and residual s_u are presented in Figure 4. More basic engineering properties of the clay are summarized in Table 3.

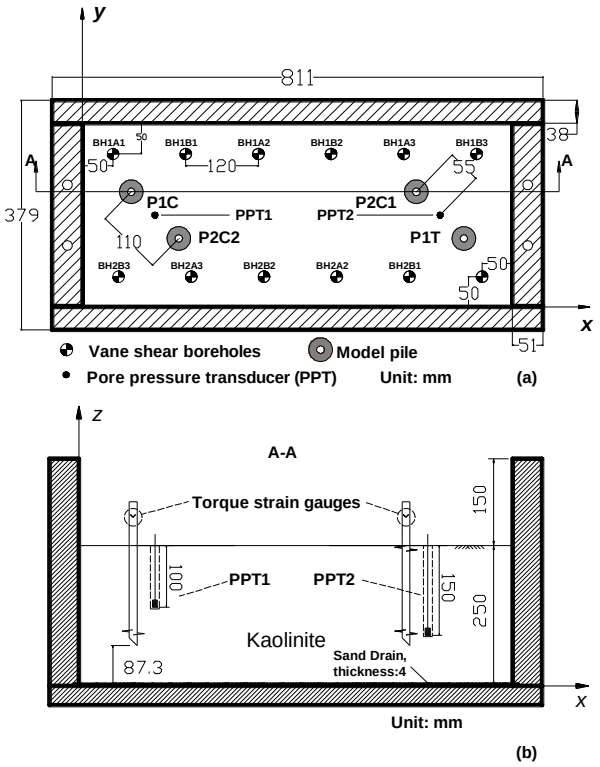

Figure 3. Test arrangement: (a) plan view and (b) vertical view.

3.5 Test Setup

As shown in Figure 5, an aluminum box with internal dimensions of 709.2 mm × 300 mm × 400 mm (height) was fabricated to contain the clay. A dual-axis electric actuator was fixed on to the top of the soil container. This actuator is able to output designated vertical and horizontal movements. The vertical movement was driven by the "vertical movement carrier". A constant-RPM motor (22.3 rpm) was fixed to the carrier and grabbed the head of a model pile.

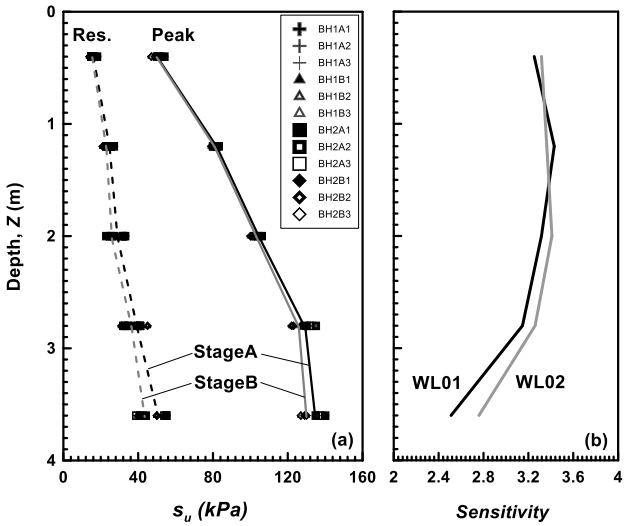

Figure 4. Peak and residual s_u of the clay

During the pile installation, the vertical movement carrier brought the motor downward at a constant penetration rate of 4.72 mm/s and at the meantime the motor exert constant rate of rotation at 22.3 rpm onto the model pile. As a result the pile was screwed into the clay at the rate of one pitch per revolution thus minimized the soil disturbance. A round disc was attached to the pile shaft about 25 mm under the torque strain gauges to stop the wires from being dragged by the high gravitational force during spinning.

The motor was replaced by an adaptor before the axial load tests since the shaft of the motor could not sustain high axial force. Then the carrier applied constant penetration rate to the pile via the adaptor. The axial movement was terminated when axial failure of the pile was observed.

Table 3. Clay properties and critical parameters in soil consolidation

G_s	PL	LL	e_0	w_0	σ_{max}	σ_{end}	e_e	w_e	γ_{sat}
2.65	33.8	54.6	2.12	80%	1500 kPa	50 kPa	0.97	36.7%	18.0 kN/ m^3

Note: G_s is specific gravity, LL is liquid limit, PL is plastic limit, e_0 is initial void ratio of the clay slurry, w_0 is initial water content of the clay slurry, σ_{max} is the maximum consolidation pressure applied to the clay slurry, σ_{end} is the last consolidation pressure after unloading, e_e is the void ratio of the prepared clay, w_e is the water content of the prepared clay, and γ_{sat} is the saturated unit weight of the prepared clay.

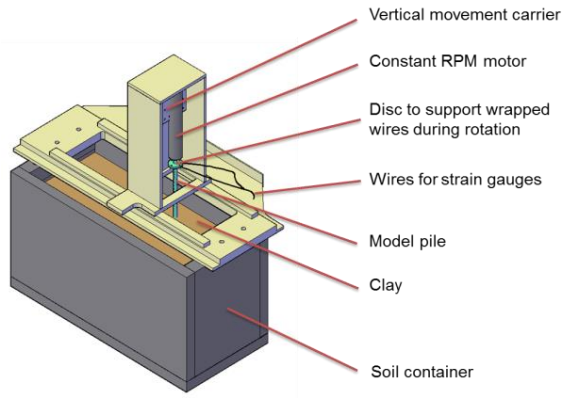

Figure 5. Equipment of installation and axial loading

4 TEST RESULTS AND DISCUSSION

The installation torques and pore pressure during pile installation were recorded and converted into prototype engineering units.

4.1 Installation Torque and Axial Capacity

The recording of the pile installation torque was started at the moment the cutting edge of the lower helix penetrated into the clay. The penetration depth, Z_h, of the pile was therefore defined as the depth of the cutting edge of the lowermost helix. The measurements of the SG's at pile head were converted into torques and presented against Z_h in Figure 6 in prototype scale. Unfortunately the wires of P2 were accidently ripped off before installation so that the installation torque of P2 was not obtained. Nevertheless, P2 was expected to show the same torque-depth behavior as P1 before the upper helix of P2 touched the clay. Prediction of the installation torque is also presented with dashed lines in Figure 6 for comparison.

The measured installation torque agreed with the estimation based on residual undrained shear strength. Therefore it is reasonable to claim that sur governed the behavior of the helical piles during installation. Since sensitivity various among different types of clay, the torque-based design method should be modified in regard to clay categories.

The axial load-displacement curves are presented in Figure 7. The measured axial capacity of P1C is significantly higher than that of P1T. In general, the bearing factor and breakout factor of a "deeply buried anchor", which usually means the embedment depth of the anchor is 5 times greater than the diameter (Das 1980), are approximately equal in cohesive soils. Otherwise, the breakout factor is expected to be smaller than the relative bearing factor. In the present study, the lower helices were embedded into the depth of 3.9 D. Therefore difference has been made between the bearing capacity and uplift capacity of these helices whereas the installation torque will not change with loading directions. Apparently, the torque factor based design method must treat bearing capacity and uplift capacity of helical piles differently when the embedment depth is considered as "shallow".

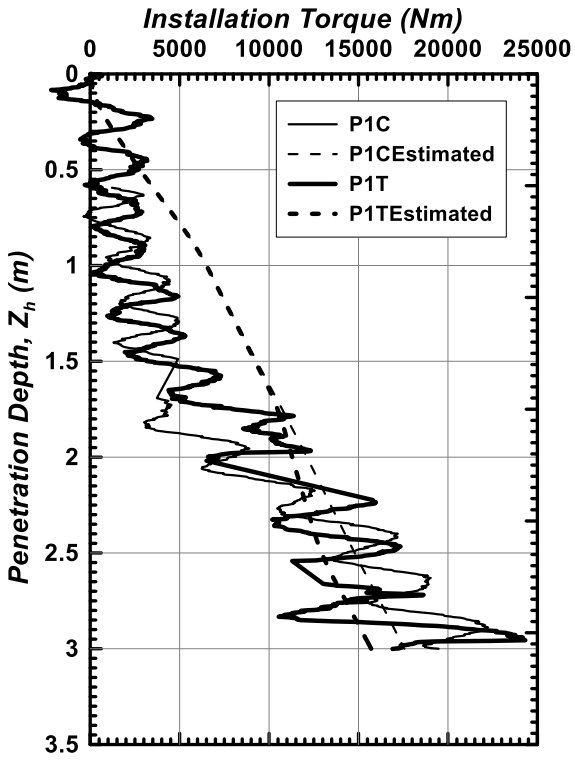

Figure 6. Installation torque vs. penetration depth

Figure 4 implies that the peak undrained shear strength of the clay slight decreased from Stage A to Stage B of the test. Therefore the axial bearing capacity of P2C1 is also slightly greater than P2C2. These measured axial capacities fall in the range of 10% off the corresponding prediction based on the measured peak undrained shear strength the end bearing factor proposed by Meyerhof (1976), shallow foundation bearing capacity of Terzaghi (1943), uplift breakout factor summarized in Das (1980), and the ineffective length proposed by Rao et al. (1993) and Li et al. (2018).

The torque factor is 31.6 m-1, 33.3 m-1, 32.5 m-1, and 20.2 m-1 for P1C, P2C1, P2C2, and P1T, respectively. According to Li and Deng (2019), the torque factor of helical piles with relevant shaft diameter to the present study is approximately 10 m-1. The discrepancy may be attributed to the high sensitivity because of high over-consolidation ratio of the clay.

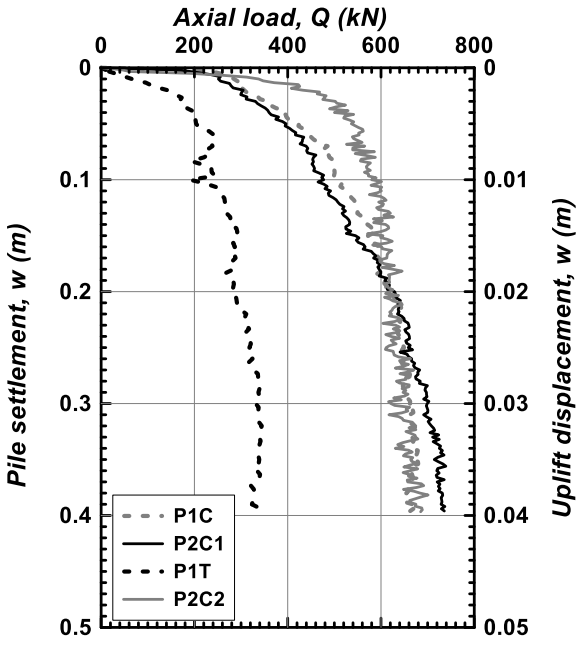

Figure 7. Axial load vs. displacement curves, in the prototype scale

4.2 Excess Pore Pressure

Excess pore pressure may cause a significant reduction of axial resistance of helical piles in clay according to Lanyi and Deng (2019), in which the bearing capacity of helical piles that were loaded immediately after installation was observed to decrease by about 30% to 40%. Figure 8 shows the excess pore pressure induced by pile installation. The peak value of the excess pore pressure was approximately 20% to 30% of the hydrostatic pore pressure. The dissipation was completed within 30 min after installation. In the prototype scale, it is equivalent to 7 days. Considering the overnight spinning time between pile installation and axial load tests, the impact of excess pore pressure on the axial capacity of these piles is negligible. In fact, the axial capacity of these tested piles was governed by s_u rather than s_{ur} according the previous discussions.

As for the excess pore pressure induced by axial loading, the PPT's did not observe notable change of pore pressure. This might be because the deformation and displacement of the clay during axial loading was local thus had limited impact on the PPT which was 8.7d away from the axis of a nearest pile.

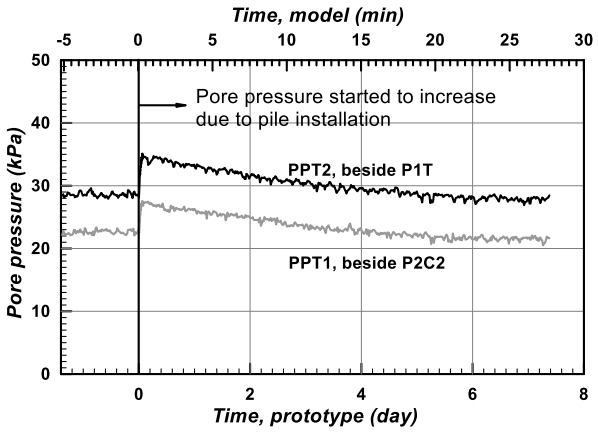

Figure 8. Excess pore pressure induced by pile installation

5 CONCLUSIONS

Eight installation and axial load tests of helical were performed on the geotechnical centrifuge at the University of Alberta. The installation torque, axial force, and excess pore pressure induced by the pile installation were obtained. Based on the test results of four selected piles, the following conclusions can be drawn:

1. The installation torque of helical piles in the stiff clay was determined by the residual shear strength whereas the axial capacity was governed by the peak undrained shear strength.

2. Since sensitivity various among different types of clay, the torque-based design method may be changed with the clay types. Highly overconsolidated clay may produce large torque factors.

3. Pore pressure response suggests that one week of recovery time should be allowed for the soil disturbed in pile installation before applying load.

6 ACKNOWLEDGEMENTS

This project was funded by the NSERC under the Collaborative R&D program (CRDPJ 485776-15) and Almita Piling Inc. The authors appreciate the assistance of Gonzalo Zambrano, Yazhao Wang, Jakob Brandl, and Gilbert Wong, staff of GeoCERF centrifuge lab facilities at the University of Alberta. Development of the centrifuge lab facilities was supported primarily by the Canada Foundation for Innovation.

7 REFERENCES

Canadian Foundation Engineering Manual (CFEM). 2006. *Canadian Geotechnical Society*.

Das, B. M. 1980. A procedure for estimation of ultimate uplift capacity of foundations in clay. *Soils and Foundations*, 20(1): 77-82.

Lanyi-Bennett, S. A., and Deng, L. 2019. Axial load testing of helical pile groups in glaciolacustrine clay. *Canadian Geotechnical Journal*, 56(2): 187-197.

Li, W., and Deng, L. 2019. Axial load tests and numerical modeling of single-helix piles in cohesive and cohesionless soils. *Acta Geotechnica*, 14(2): 461-475.

Li, W., Zhang, D. J. Y., Sego, D. C., and Deng, L. 2018. Field testing of axial performance of large-diameter helical piles at two soil sites. *Journal of Geotechnical and Geoenvironmental Engineering*, 144(3): 06017021.

Meyerhof GG. 1976. Bearing capacity and settlement of pile foundations. *J Geotech Eng Div ASCE* 102(3):195–228

Rao, S. N., Prasad, Y. V. S. N., and Veeresh, C. 1993. Behaviour of embedded model screw anchors in soft clays. *Geotechnique*, 43(4): 605-614.

Sakr, M. 2009. Performance of helical piles in oil sand. *Canadian Geotechnical Journal*, 46(9): 1046-1061.

Sakr, M. 2012. Torque prediction of helical piles in cohesive soils. In Proc., *65th Canadian Geotechnical Conf.*(CGC). Richmond, BC, Canada: *Canadian Geotechnical Society.*

Sakr, M. 2013. Relationship between installation torque and axial capacities of helical piles in cohesive soils. *DFI Journal-The Journal of the Deep Foundations Institute*, 7(1): 44-58.

Spagnoli, G., de Hollanda Cavalcanti Tsuha, C., Oreste, P., and Mendez Solarte, C. M. 2018. A sensitivity analysis on the parameters affecting large diameter helical pile installation torque, depth and installation power for offshore applications. *DFI Journal-The Journal of the Deep Foundations Institute*, 12(3): 171-185.

Tappenden, K. M., and Sego, D. C. 2007. Predicting the axial capacity of screw piles installed in Canadian soils. In The *Canadian Geotechnical Society (CGS), OttawaGeo2007 Conference*: 1608-1615.

Terzaghi, K. 1943. *Theoretical soil mechanics*. 5th Ed., John Wiley and Sons Inc., New York, N.Y.

Tsuha, Cristina de Hollanda Cavalcanti, and Nelson Aoki. 2010. Relationship between installation torque and uplift capacity of deep helical piles in sand. *Canadian Geotechnical Journal*, 47(6): 635-647.